



Wind speed deviations in complex terrain

Christian Ingenhorst^{1/3}, Georg Jacobs¹, Laura Stöbel², Ralf Schelenz², Björn Juretzki³

¹Institute for Maschine Elements and Systems Engineering, Aachen, 52062, Germany

²Center for Wind Power Drives, RWTH Aachen, Aachen, 52074, Germany

5 ³IME Aachen GmbH Institut für Maschinenelemente und Maschinengestaltung, Aachen, 52074, Germany

Correspondence to: Christian Ingenhorst (christian.ingenhorst@imse.rwth-aachen.de)

Abstract. Wind farm sites within complex terrain are subject to local wind phenomena, which have a huge impact on a wind turbine's annual energy production. To reduce investment risk, an extensive site evaluation is therefore mandatory. Stationary long-term measurements are supplemented by CFD simulations, which are a commonly used tool to analyse and understand the three-dimensional wind flows above complex terrain. Though being under heavy research, such simulations still show a huge sensitivity for various input parameters like terrain, atmosphere and numerical setup. Within this paper, a different approach aims to *measure* instead of simulate wind speed deviations above complex terrain by using a flexible, airborne measurement system. An unmanned aerial vehicle is equipped with a standard ultrasonic anemometer. The uncertainty of the system is evaluated against stationary anemometer at different heights and shows very good agreement, especially in mean wind speed ($<0.12 \text{ ms}^{-1}$) and mean direction ($<2.4^\circ$) estimation. A test measurement was conducted above a forested and hilly site to analyse the spatial and temporal variability of the wind situation. A position dependent difference in wind speed increase up to 30 % compared to a stationary anemometer is detected.

1 Introduction

Complex and mountainous terrain gains importance for wind farm development due to land use conflicts and a high wind potential by speed-up effects at escarpments and steep ridges. Nevertheless, such orographic features as well as obstacles, roughness differences and jet/tunnel effects result in a complex wind field, increase the risk of annual energy production (AEP) overestimation as it was pointed out by (Lange et al., 2017). Within a wind farm in complex terrain, that was analysed by (Ayala et al., 2017), the AEP of single wind turbines varied up to 25 %, although wake effects seem to be neglectable when taking into account the park layout and prevailing wind directions.

25 An increasing demand of renewable energy and high investment risks in case of a false AEP prognosis make wind flows in complex terrain an intensively investigated research topic, concerning both measurement and simulation. Computational Fluid Dynamics (CFD) simulations are a common tool to investigate the spatially distributed wind speeds above complex terrain and is widely used in site assessment. Although huge advances in computational power allow even more detailed flow simulations in recent years, CFD simulations still show great sensitivity for assumptions and simplifications such as terrain details and surface roughness (Jancewicz and Szymanowski, 2017; Lange et al., 2017), atmospheric stability (Koblitz et al.,



2014), turbulence models (Tabas et al., 2019) aside of various numerical parameters. Remaining uncertainties and long computation times make measurements for sites in complex terrain mandatory for a bankable site assessment. This is also taken into account by various guidelines (International Electrotechnical Commission, 2009; Measnet, 2016; Fördergesellschaft Windenergie und andere Dezentrale Energien, 2017).

35 Nevertheless, guideline-compliant measurement equipment such as met masts and LIDARs are operated stationary with a focus on a maximum statistical coverage. Such systems are not applicable to investigate the spatial deviation of wind speeds within a certain area. A state-of-the-art measurement approach is the combination of several scanning LIDARs to measure a 3D wind field. Such systems were successfully used to detect and analyse wind phenomena in several experiments, from wind tunnel (van Dooren et al., 2017) to full scale experiments (Pauscher et al., 2016; Vasiljević et al., 2017). However, scanning
40 LIDARs are rather costly and have a reasonable installation effort, especially in steep and forested terrain when line of sight matters. This topic gets even more important, when the planned measurement campaign requires careful positioning of the single LIDAR systems to avoid increasing measurement errors (Stawiarski et al., 2013).

Within this paper, a different approach towards a *measured* 3D wind field is presented, based on a measurement strategy with a multi-rotor unmanned aerial vehicle (UAV) equipped with an ultrasonic anemometer (USA). Autonomous UAVs, especially
45 fixed-wing systems with pitot-based wind sensors, have been used for atmospheric research since the last 20 years (Holland et al., 2001; Spiess et al., 2007; Reuder et al., 2009). In opposite to fixed-wing UAVs, which have a minimum necessary flight speed, rotary-wing aircrafts can hold their position mid-air for several minutes of measurement. Such systems already showed promising results for single wind measurements in (Bergmann et al., 2017; Palomaki et al., 2017; Vasiljević et al., 2019), but have not yet been used to investigate spatial deviations of wind speeds and directions above complex terrain.

50 The investigation described within this paper was performed with a commercial full-scale 3D USA mounted on a multi-rotor UAV. The measurement system is highly portable and offers great flexibility, allowing USA measurements over any kind of terrain. However, two challenges have to be met to establish airborne measurements as an alternative to common CFD simulations for investigating complex flow fields:

1. The surrounding air (and its fluctuation) is the measured variable, but at the same time working medium and
55 disturbance for the flying carrier system. Movements and rotations of the UAV as well as rotor induced flows have a significant impact on the measured wind speed, direction and turbulence intensity. Measurement accuracy therefore has to be validated and is discussed in Section 2 of this paper.
2. CFD Simulations offer the possibility to investigate the 3D wind field at each calculation point for every single time step. The UAV instead measures one point after another and takes considerable time in doing so. The challenge is to
60 separate the measured wind speed deviations into spatial deviations (due to complex topography) on the one hand and temporal deviations (due to changes of the general wind situation) on the other hand. In Section 3 of this paper, a first approach including a stationary reference is evaluated and discussed.



2 Measurement System “WindLocator”

65 2.1 Design

The measurement system, which has been used for the measurement campaigns within this paper, has two main, independent components: a powerful carrier system and a sensor unit, which consists of a commercially available ultrasonic anemometer and a self-developed compensation and data acquisition unit.

70 The foldable, commercial carrier system is a battery powered octocopter with a flight time of 25 mins and a maximum take-off-weight of 12.5 kg. Including the sensor unit, the complete system only weighs 8.5 kg and therefore has a considerable performance reserve. Flights at turbulent air as well as during gust speeds of 25 ms^{-1} have successfully been tested. A real-time-kinematics (RTK) GPS is included to perform high accuracy positional navigation and speed estimation. The open source flight controller has been adapted for an easy setup of specific measurement strategies, which then are autonomously being followed. Although a completely unobserved operation is technically possible, European laws at this moment require an
75 operator to be within sight.



Figure 1: Measurement system WindLocator (unfolded) without battery packs

Table 1 Specifications of carrier system

Dimensions	1060mm (diameter motor-motor), 1250mm (height)
Weight (incl. sensor unit)	8,5 kg



Maximum take-off weight	12 kg
Rotors	8 x 385mm carbon fibre reinforced polymer rotors
Battery	2 x 10.000 mAh
Flight Controller	Pixhawk Cube
Flight Times (incl. sensor unit)	~25 mins
Air speed	10 ms ⁻¹

- 80 The Gill WindMaster 3D ultrasonic anemometer is placed on top of the compensation unit centred above the rotor plane. Mounting the sensor on top of the UAV has several advantages. First of all, the rotational symmetry of the system allows wind measurement independent from yaw angle and wind direction. Additionally, this setup results in a horizontally centred mass during hovering and therefore leads to relatively small moments to be compensated by the UAV. This improves flight performance and flight time. Aside of that, the downwash above the rotors is less turbulent than below.
- 85 The distance of the sensor's measurement volume to the rotor plane is 750 mm and is considered as a trade-off between manoeuvrability and reasonable interaction between wind sensor and propeller induced flows.

Table 2 Specifications of the ultrasonic anemometer

Type		Gill WindMaster 1590-PK-020
Wind Speed	Range	0-50 ms ⁻¹
	Resolution	0.01 ms ⁻¹
	Accuracy	< 0.18 ms ⁻¹
Direction	Range	0-359°
	Resolution	0.1°
	Accuracy	2° @ 12 ms ⁻¹
Measurement	Internal sample rate	20 Hz

- 90 Except for the power supply, the self-developed compensation and data acquisition unit is completely independent from the UAV. If requirements concerning the carrier system change, the compensation unit as a whole can be reapplied easily on a new aircraft. It weighs 420 gr and contains all necessary sensors as well as an additional RTK-GPS for an accurate position and speed estimation by means of sensor fusion. Based on analytical calculations and various synthetic experiments, a compensation algorithm was developed, that efficiently reduces measurement errors due to movements of the airborne system
- 95 as well as its rotors. Additional telemetry transmits measurement data such as wind speeds and directions live to a ground station for in situ analysis. The anemometer data is additionally saved to an internal storage with a rate of 10 Hz.



2.2 Validation of the system

100 All following calculations and measurements have been evaluated based on data, that has been processed by the compensation unit. The system validation in general was conducted on several levels of detail, beginning with the Guide to the Expression of Uncertainty in Measurement (GUM) to evaluate the standard uncertainty of a single measurement datum. The GUM allows the calculation of the standard uncertainty without the necessity of a true reference value. Error estimation is done by creating a mathematical model of the WindLocator, including relevant influences and their uncertainties and combining them into the system's standard uncertainty, which is $\pm 0.37 \text{ ms}^{-1}$ in our case.

105 After several synthetic tests with a fixated UAV to evaluate rotor influences (Figure 2), the WindLocator's compensation unit was tested during an indoor flight at zero-wind conditions (Figure 3).

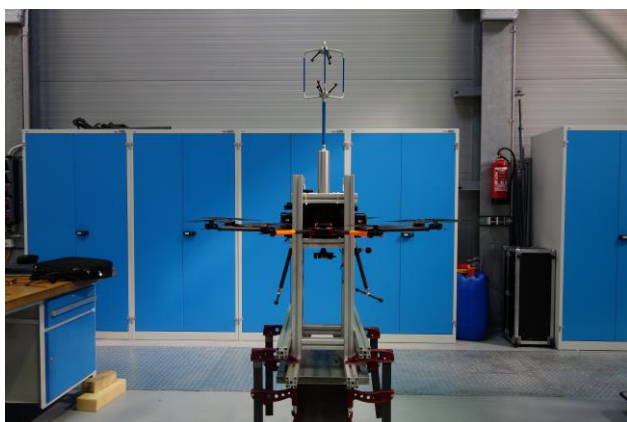


Figure 2 fixed UAV



Figure 3 Indoor flight at zero-wind conditions

110 Because no stable GPS signal could be received during the indoor flight, the WindLocator was set to “Altitude Hold”, which utilizes the internal barometer to maintain an altitude of around 4 m during our test and automatically stabilizes pitch and roll axis for minimum horizontal movements. Nevertheless, small sensor inaccuracies made pilot interventions necessary to remain at sufficient distance to walls. After compensation, the wind data is given out in a global north-east-down coordinate system and is therefore independent from the specific orientation of the UAV.

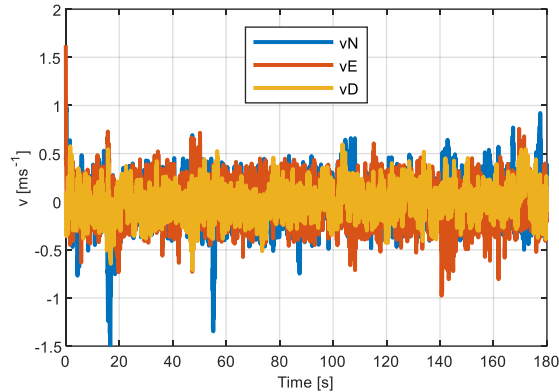


Figure 4 North-East-Down wind speed components of indoor flight at zero wind conditions

Figure 4 shows the data in all three measured directions at a resolution of 10 Hz. Peaks, e.g. in vN-direction at second 17 (-1.5 ms^{-1}) and 55 (-1.31 ms^{-1}) are a result of the UAV’s horizontal translation due to operator intervention.

115 **Table 3: Results of measured wind speed components during indoor flight**

	Wind speed north (vN)	Wind speed east (vE)	Wind speed down (vD)
Mean value [ms^{-1}]	0.01	-0.02	0.00
Standard deviation [ms^{-1}]	0.23	0.21	0.16

As expected, mean wind speeds during the indoor flight are very close to zero. Standard deviations up to 0.23 ms^{-1} meet our expectations according to GUM, but clearly show the influence of manual operator control and of the sensor being rather close to the turbulent downwash induced by the rotors.

120 After showing that under zero-wind conditions, mean values are in good agreement with our expectations, a measurement setup was created to compare the performance of the WindLocator with a stationary anemometer. In flat, agricultural terrain 2 km west of Aachen (Northrhine-Westfalia, Germany), a stationary anemometer of the same type as the UAV’s anemometer was mounted at a height of 3 m above ground level. Data acquisition and storage for the stationary anemometer were realised at 10 Hz by a self-developed data acquisition system, which uses time stamps synced with an internet time server. The UAV
 125 time stamps are derived from GPS time signals. The UAV was set to hold position at a height of 3 m. A distance of 4 m to the stationary anemometer rectangular to the main wind direction was chosen to avoid interactions of the two measurement systems (Figure 5).



Figure 5 WindLocator hovering close to stationary anemometer

130 Four ten-minute measurements with ~6000 data points each have been conducted, with a short break to switch batteries after the second measurement point. In opposite to the indoor tests, all three wind components are combined into a single wind speed v for every measurement datum to improve comparability to the stationary anemometer. However, the vertical component v_D in general has a minor impact on the resulting wind speeds.

$$v = \sqrt{v_N^2 + v_E^2 + v_D^2}$$

135 The following diagrams (Figure 6-Figure 9) show the compensated wind speeds of the WindLocator in comparison to the stationary reference as well as the corresponding regression plot.

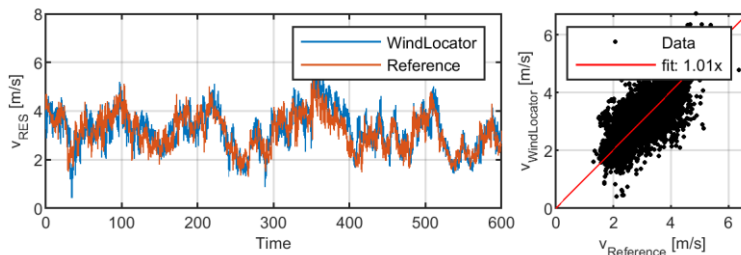


Figure 6: resulting ground level wind speed and regression plot of measurement 1

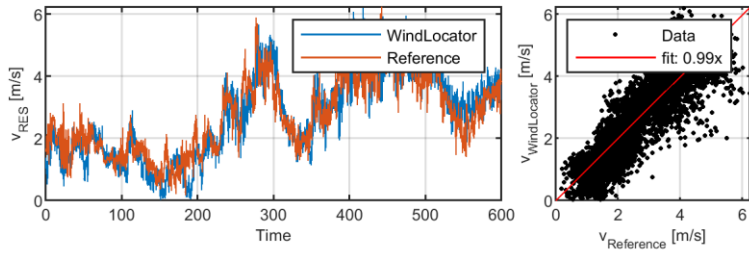


Figure 7: resulting ground level wind speed and regression plot of measurement 2

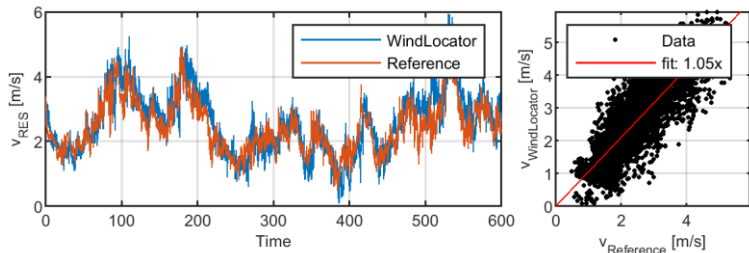


Figure 8: resulting ground level wind speed and regression plot of measurement 3

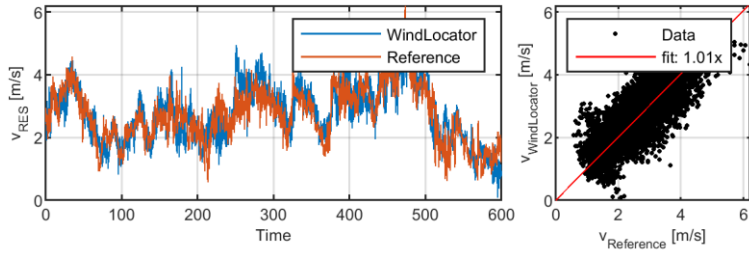


Figure 9: resulting ground level wind speed and regression plot of measurement 4

145 For all measurement points (see Table 4), a very good agreement of the ten-minute-mean wind speed between WindLocator and reference has been achieved, especially when taking into account the turbulent wind situation during such a low-altitude flight. Turbulence intensities (TI) up to 44 % have been calculated for the stationary reference. Although there are absolute differences of +1 % (measurement 1) to +6 % (measurement 2/4), the WindLocator already gives a good estimation of the prevailing turbulence intensity.

150 **Table 4 Comparison of measurement points on ground level**

	Measurement 1	Measurement 2	Measurement 3	Measurement 4
Mean speed difference [ms ⁻¹]	-0.07	-0.12	-0.06	0.02
TI Reference [%]	24,5%	32,2%	32,2%	44,3%



TI UAV [%]	25,1%	37,7%	32,8%	50,2%
R²	0.53	0.69	0.63	0.78
Standard deviation [ms⁻¹]	0.58	0.55	0.58	0.64

An analysis of wind directions during this experiment was not yet possible, because an accurate orientation of the stationary measurement system could not be guaranteed. This is taken into account for the next experiment at a 134 m met mast under more realistic conditions (Figure 10).



Figure 10: 134 m met mast at Windtest Grevenbroich GmbH test site in Germany

155

160

The measurement system was tested on a sunny day close to a met mast on a small plateau. Four measurements of 8-10 minutes have been conducted and are compared to the velocity data of a cup anemometer at 134 m and the directional data of a wind vane at 130 m above ground level. The WindLocator was flown to a height of 134 m based on barometer and GPS data and was then moved closer towards the met mast using the onboard camera system. Because the flight was performed without autopilot, distances to the met mast and exact height vary throughout the measurements (see Table 5). Additionally, that table contains wind speed data analogue to Table 4 as well as information concerning the accuracy of wind direction estimations. For all following calculations, the WindLocator data was averaged to 1 Hz for better comparability to the met mast.

Table 5: Comparison of measurements on 134m

parameter	Measurement 1	Measurement 2	Measurement 3	Measurement 4
Distance to met mast [m]	26	24	17	16
measurement height [m _{agl}]	134	133	135	135



Mean speed difference [ms^{-1}]	-0.21	0.01	0.20	-0.06
TI Reference [%]	15.1	18.5	11.8	15.1
TI UAV [%]	13.4	17.2	12.3	15.2
R^2	0.28	0.49	0.44	0.80
Standard deviation [ms^{-1}]	0.88	0.88	0.63	0.47
mean angular difference [$^\circ$]	1.2	-0.7	2.0	2.4
R^2	0.56	0.49	0.82	0.71
Standard deviation [$^\circ$]	8.5	10.8	5.1	4.6

165

The results during the met mast experiment show a slightly different picture compared to the ground level measurements. Still comparable to the former test is the reasonable performance of the turbulence intensity estimation of the UAV. Additionally, measurements 2 (Figure 12) and 4 (Figure 14) show a good correlation of the WindLocator and the corresponding reference speed. However, mean wind speed deviations for the first and third measurement are not only higher than before, but also vary a lot more compared to the other measurements of that day. Serious deviations mainly occur during the first half of the measurements (Figure 11; Figure 13) in a temporary manner, e.g. seconds 180 to 270 for measurement 3.

170

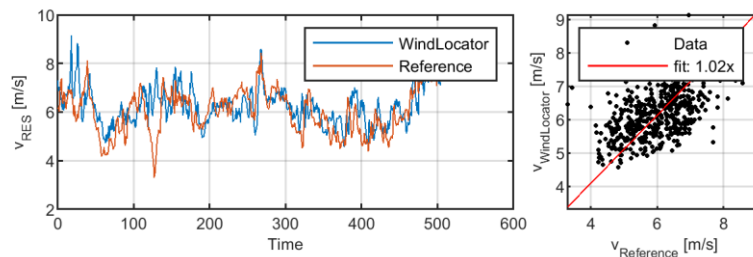


Figure 11: resulting wind speed at 134m and regression plot of measurement 1

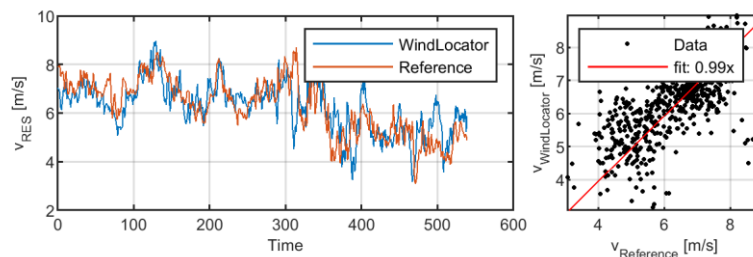


Figure 12: resulting wind speed at 134m and regression plot of measurement 2

175

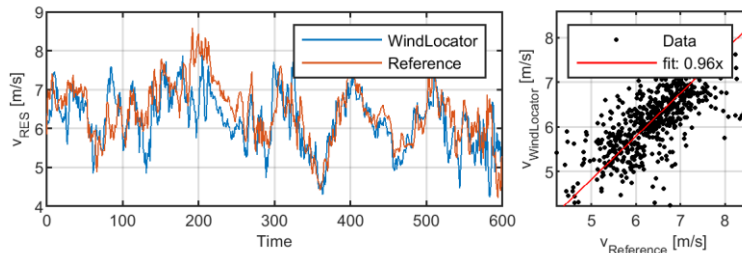


Figure 13: resulting wind speed at 134m and regression plot of measurement 3

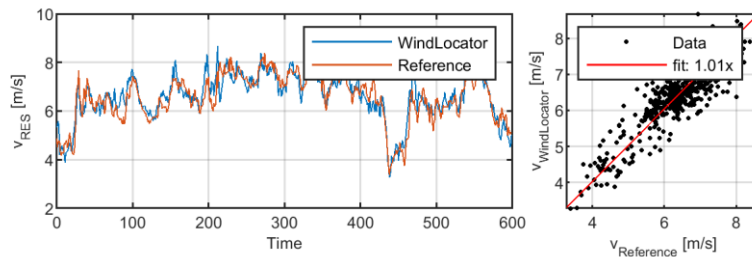


Figure 14: resulting wind speed at 134m and regression plot of measurement 4

180 Those deviations are a result of the pilot still doing positional adjustments during the measurement point. Nevertheless, those adjustments seem not to have a critical impact on the UAV's wind direction estimation, which shows very good correlation through all measurement points with a maximum mean deviation between met mast and WindLocator of 2.4° . Absolute wind directions and their regression plots are shown in Figure 15-Figure 18.

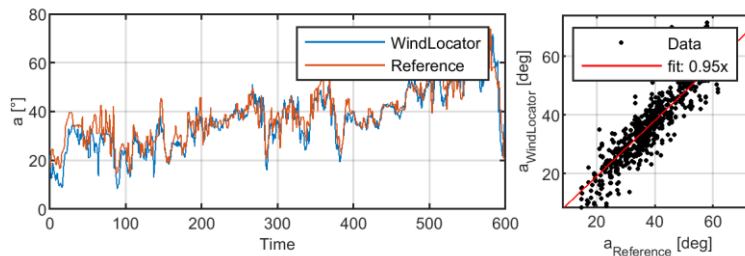


Figure 15: wind direction at 134m and regression plot of measurement 1

185

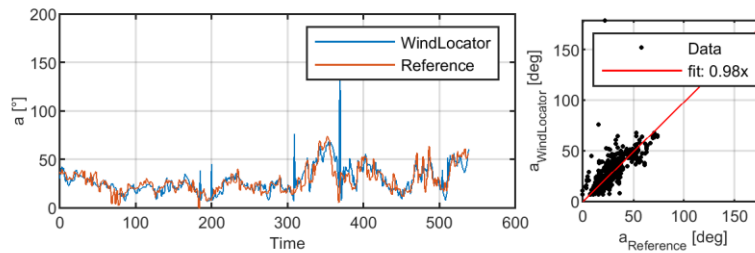


Figure 16: wind direction at 134m and regression plot of measurement 2

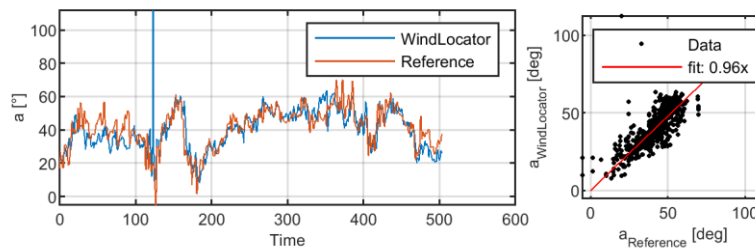


Figure 17: wind direction at 134m and regression plot of measurement 3

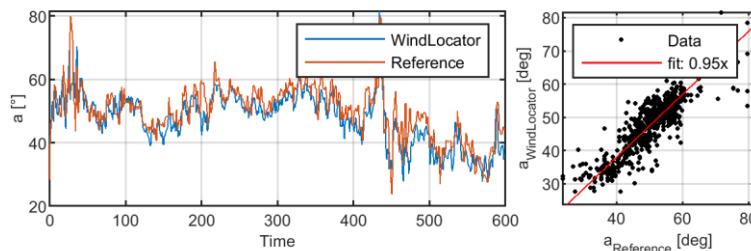


Figure 18: wind direction at 134m and regression plot of measurement 4

190

Despite its challenging but beneficial design with the anemometer mounted above the rotor plane, the WindLocator performed very well throughout the tests, especially concerning the calculation of averaged measurement quantities like speed and direction. When the system uses its GPS based hover mode without “disturbance” by a pilot, mean wind speed differences compared to a reference were below 0.12 ms^{-1} and wind direction differences smaller than 2.4° . Because the
195 airborne measurement system and a reference cannot measure at the exact same place at the exact same time, remaining uncertainties always also might be a result of spatial deviations in the wind situation, which will be discussed in more detail in the following section.



3.1 Test site and measurement setup

200 The aim of the campaign is to investigate mean wind speed deviations above complex terrain by using the WindLocator. The area for this measurement campaign is a small hill in the south of Northrhine-Westphalia in the german Eifel and was chosen for the following reasons:

- With a yearly mean wind speed of $6.5-7 \text{ ms}^{-1}$ at 100 m above ground level, the area has rather high wind speeds compared to the rest of the county. Main wind direction is southwest.
- The terrain is considered to be complex (Figure 19). The slope around the hill at most parts is greater than 40 degrees. Forests extend to the south and west of the hill. A small village is located to the northeast.
- The region in general was considered to be suitable for wind turbines and has a good accessibility.

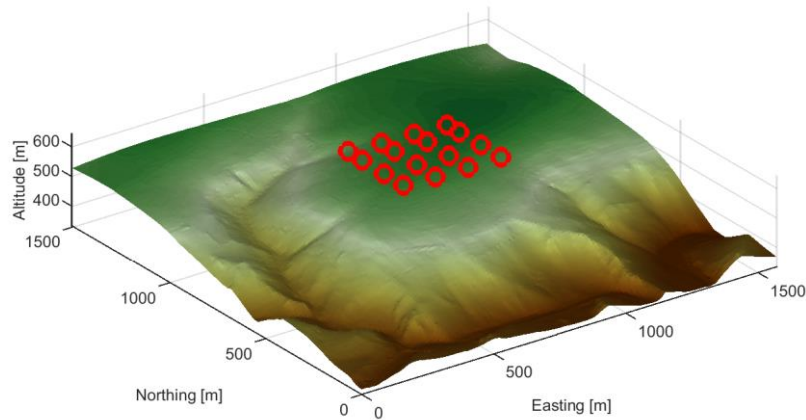


Figure 19 terrain model of the test area and measurement points (red)

210 To reduce experimental complexity, wind speed deviations within a two-dimensional plane above the described complex landscape are going to be investigated. The plane to be surveyed is roughly 500 m x 500 m and placed on the middle of the hill with equal distance to the edges in the south and west. All planned measurement points, which are displayed as red circles in Figure 19, are at the same height above sea level and around 100 m above the lift-off point. Additional information is summarized in Table 6.

215 **Table 6: Summary of the measured plane**

Number of points	16 (4 x 4)
Distance between points	~ 120 m
Measurement time per point	5 mins



Measurement rate	10 Hz
Measurement points per battery charge	4

The measurement workflow begins with the activation of the WindLocator's autopilot. The system then automatically flies to the first, predefined measurement point and holds position for five minutes before heading for the next point. For this feasibility study, five minutes were considered to be a reasonable trade-off between limited battery time and statistical coverage for each measurement point. After four measurement points, the UAV automatically returns to its lift-off position for a battery change. Afterwards, the measurement process continues with the next point. During post-processing, measurement points are automatically detected within the data for further analysis.

Aside of the WindLocator, an additional stationary ultrasonic anemometer was in use during the campaign. It was placed at a height of 3 m on free grassland, nearly centred under the measurement plane and also acquires data at 10 Hz.

3.2 Results

Figure 20 gives an overview of the measured resulting wind speeds v from the moving WindLocator and the stationary reference on ground. After the data acquisition was started, the UAV heads for the first measurement point, where it is holding position for five minutes 100 m above ground, before heading for the next waypoint. A measured wind speed deviation between WindLocator and reference is expected because of the differences in height and horizontal position of both systems. During the battery swap after four measurement positions, obviously no WindLocator data is available. The stationary reference instead measures non-stop. Measuring 16 points of five minutes, making it 80 minutes of usable measurement data, has taken around two hours in total.

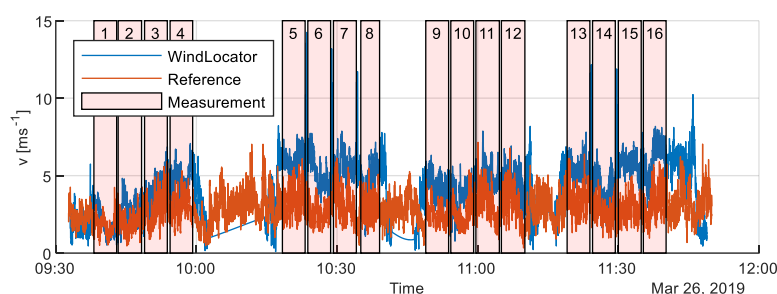


Figure 20: Comparison of resulting wind speeds from WindLocator (compensated) and Reference at 10Hz

Over all UAV measurement points, an absolute variation of mean wind speeds between 2 and 6 ms^{-1} has been detected (Figure 21). As it was already implied in the introduction, this obviously is not only a result of spatial deviations due to complex terrain, but also a consequence of wind variation over time. Otherwise, the stationary reference (assuming it to be an indicator for the overall wind situation) would not have shown any significant differences in wind speed over time.

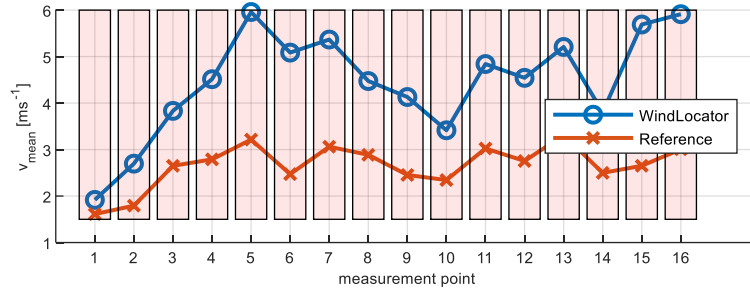


Figure 21: absolute mean wind speeds of WindLocator and reference

240

This is clearly not the case, especially when looking at the normalised reference wind speed, calculated by dividing the mean wind speed value of each point by the maximum mean value of all measurement points (Figure 22). The strong correlation (R=0.86) between relative mean speeds of WindLocator and reference data is an indicator, that the ground level stationary anemometer for this particular campaign is a suitable reference to also track temporal changes of the overall wind situation.

245

The remaining differences between WindLocator and reference tend to be local wind speed deviations, e.g. due to terrain.

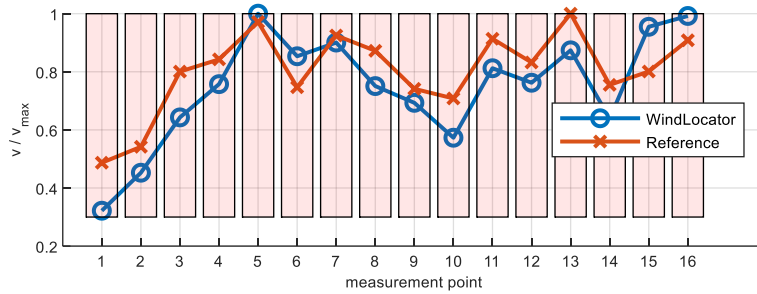


Figure 22: normalized mean wind speeds of WindLocator and reference

Taking this into account, a very simple measurement strategy seems suitable as a first approach: the time offset between single UAV measurement points can be compensated by referencing them to the stationary anemometer data. The result is a measured wind speed increase compared to the reference and is summarized in Table 7.

250

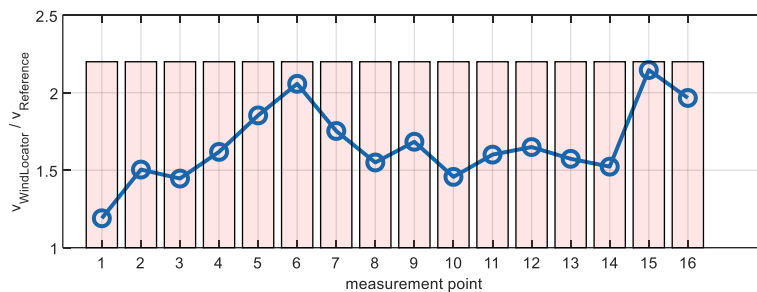


Figure 23: wind speed increase from reference to WindLocator

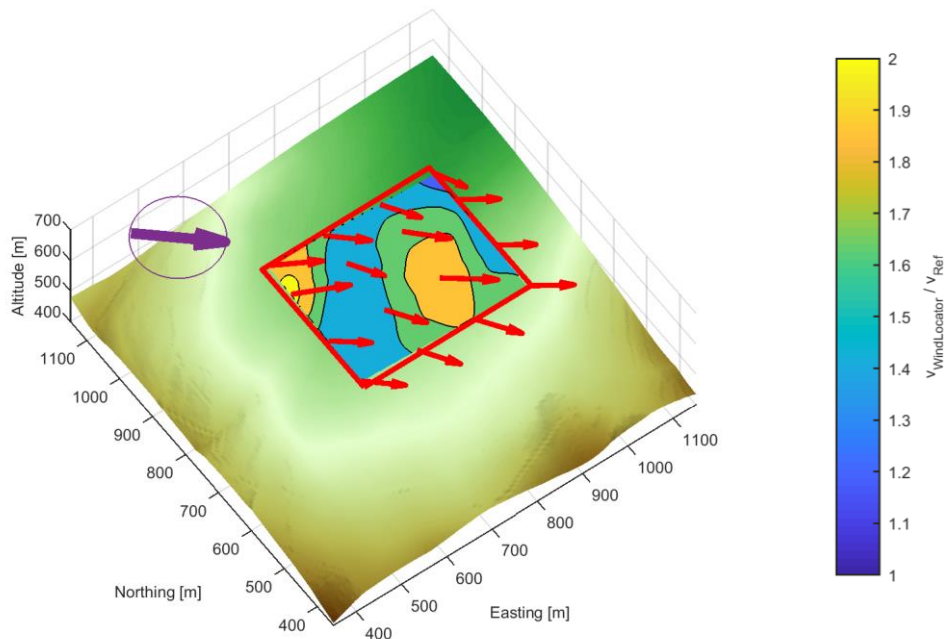


255 **Table 7 wind speed increase compared to reference**

Mean	1.66
Maximum	2.15 (+30% compared to mean value)
Minimum	1.19 (-28% compared to mean value)
Standard deviation	0.25 (15% of mean value)

This measurement strategy, nevertheless, depends on various parameters concerning the stationary reference, its positioning and expected spatial variations and therefore cannot be considered to be valid in general. Advanced measurement strategies and criteria are currently under development.

260 Figure 24 combines the measured results on the one hand and the UAV's GPS data on the other hand to a spatial distribution. The purple arrow indicates the mean wind direction. Each red arrow represents a measurement point, showing the measured horizontal wind direction and indicating with its length the wind speed increase compared to the stationary reference. For a better insight, the wind speed increase then is interpolated linearly between measurement points to create a contour plot. The background shows the digital terrain model data.



265

Figure 24 measured mean wind speed distribution above complex terrain



The highest increase in wind speed compared to the stationary anemometer is located towards the ridge at the upwind side, which meets our expectations concerning of a speed-up effect at a steep hill. The following area of lower wind speeds might then be a result of flow separation. Downwind of the hill, towards the southeast ridge, an additional area of higher wind speeds is located. Towards the plateau in northeast direction, lowest wind speed increase has been measured.

4 Conclusion

Within this paper, a UAV-based measurement system called WindLocator, its validation and its experimental application above complex terrain were presented. The measurement system consists of a powerful octocopter, a commercial ultrasonic anemometer centred above the rotor plane and a self-developed compensation and data acquisition unit. The latter was the enabler to efficiently reduce wind measurement errors due to movements of the UAV and rotor influences. This has been shown in two test scenarios at different wind and turbulence conditions.

At both tests, very good agreement with reference data could be achieved. Mean wind speeds have been estimated with a maximum difference of 0.12 ms^{-1} , wind directions with a maximum difference of 2.4° during position-controlled hovering. Though rotor influences are a challenge, turbulence intensity estimation was reasonably good. Nevertheless, the compensation unit is under continuous development to improve accuracy at all relevant flight situations.

The biggest advantage of an airborne measurement system is its flexibility, allowing measurements at any arbitrary point in a wind field above any kind of landscape. This could make the WindLocator to a potential alternative for CFD simulations in complex terrain, delivering an analogue result for a specific weather situation without long computation times or modelling uncertainties. To do so, temporal and spatial variations of wind speed have to separated.

A hilly and forested region in the germen Eifel is investigated concerning its local wind speed deviations by using the WindLocator. Although more advanced measurement strategies are currently under development, for this specific case, a very simple strategy was sufficient due to a good time correlation between reference and UAV: while the WindLocator automatically was flying from point to point, a stationary reference at ground level was used to compensate the time offset between single measurement points. The result was a plane of four times four measurement points, including information of wind speed increase compared to the reference and three-dimensional wind directions. Spatial differences of approximately $\pm 30\%$ compared to a mean value have been found at plausible locations, underlining the necessity of intensive site evaluation in complex terrain.

Acknowledgements

We thank Windtest Grevenbroich GmbH for providing validation data from a meteorological mast at their test site.



Competing interests

Christian Ingenhorst is PhD student at the Institute for Machine Elements and Machine Design (IMSE) and employee at the
300 IME Aachen GmbH. This company is offering airborne wind measurements as a service.

Author contributions

Christian Ingenhorst: validation, measurements and analysis

Laura Stöbel: measurement site and strategy

305 Georg Jacobs: supervision of Christian Ingenhorst and paper correction

Ralf Schelenz: supervision of Laura Stöbel

Björn Juretzki: supervision of Christian Ingenhorst and paper correction

References

- 310 Ayala, M., Maldonado, J., Paccha, E., and Riba, C.: Wind Power Resource Assessment in Complex Terrain: Villonaco Case-
study Using Computational Fluid Dynamics Analysis, *Energy Procedia*, 107, 41–48,
<https://doi.org/10.1016/j.egypro.2016.12.127>, 2017.
- Bergmann, D., Bischoff, O., Denzel, J., Cheng, P. W., Hofsäb, M., Lutz, T., Peters, B., and Schulz, C.: Entwicklung von
Lidar-Technologien zur Erfassung von Windfeldstrukturen hinsichtlich der Optimierung der Windenergienutzung im
bergigen, komplexen Gelände, Abschlussbericht des Forschungsprojektes ein Vorhaben des WINDFORS, Windenergie
315 Forschungscluster Forschungsnetzwerks Projektpartner: Universität Stuttgart, Universität Tübingen, Karlsruher Institut
für Technologie, Fördergesellschaft Windenergie, 2017.
- Fördergesellschaft Windenergie und andere Dezentrale Energien: Technische Richtlinien für Windenergieanlagen, 10th ed.,
2017.
- Holland, G. J., Webster, P. J., Curry, J. A., Tyrell, G., Gauntlett, D., Brett, G., Becker, J., Hoag, R., and Vaglianti, W.: The
320 Aerosonde Robotic Aircraft: A New Paradigm for Environmental Observations, *Bull. Amer. Meteor. Soc.*, 82, 889–901,
[https://doi.org/10.1175/1520-0477\(2001\)082<0889:TARAAN>2.3.CO;2](https://doi.org/10.1175/1520-0477(2001)082<0889:TARAAN>2.3.CO;2), 2001.
- International Electrotechnical Commission: Windenergieanlagen: Teil 12: Messung des Leistungsverhaltens von Elektrizität
erzeugenden Windturbinen basierend auf Gondelanemometrie, 2009.
- Jancewicz, K. and Szymanowski, M.: The Relevance of Surface Roughness Data Qualities in Diagnostic Modeling of Wind
325 Velocity in Complex Terrain: A Case Study from the Śnieżnik Massif (SW Poland), *Pure Appl. Geophys.*, 174, 569–
594, <https://doi.org/10.1007/s00024-016-1297-9>, 2017.
- Koblitz, T., Bechmann, A., Berg, J., Sogachev, A., Sørensen, N., and Réthoré, P.-E.: Atmospheric stability and complex
terrain: comparing measurements and CFD, *Boundary-Layer Meteorol*, 555, 12060, [https://doi.org/10.1088/1742-
6596/555/1/012060](https://doi.org/10.1088/1742-6596/555/1/012060), 2014.



- 330 Lange, J., Mann, J., Berg, J., Parvu, D., Kilpatrick, R., Costache, A., Chowdhury, J., Siddiqui, K., and Hangan, H.: For wind turbines in complex terrain, the devil is in the detail, *Environ. Res. Lett.*, 12, 94020, <https://doi.org/10.1088/1748-9326/aa81db>, 2017.
- Measnet: Evaluation of site-specific wind conditions, 2016.
- 335 Palomaki, R. T., Rose, N. T., van den Bossche, M., Sherman, T. J., and Wekker, S. F. J. de: Wind Estimation in the Lower Atmosphere Using Multirotor Aircraft, *J. Atmos. Oceanic Technol.*, 34, 1183–1191, <https://doi.org/10.1175/JTECH-D-16-0177.1>, 2017.
- Pauscher, L., Vasiljevic, N., Callies, D., Lea, G., Mann, J., Klaas, T., Hieronimus, J., Gottschall, J., Schwesig, A., Kühn, M., and Courtney, M.: An Inter-Comparison Study of Multi- and DBS Lidar Measurements in Complex Terrain, *Remote Sensing*, 8, 782, <https://doi.org/10.3390/rs8090782>, 2016.
- 340 Reuder, J., Brisset, P., Jonassen, M. M., and Mayer, S.: The Small Unmanned Meteorological Observer SUMO: A new tool for atmospheric boundary layer research, *metz*, 18, 141–147, <https://doi.org/10.1127/0941-2948/2009/0363>, 2009.
- Spiess, T., Bange, J., Buschmann, M., and Vörsmann, P.: First application of the meteorological Mini-UAV 'M2AV', *metz*, 16, 159–169, <https://doi.org/10.1127/0941-2948/2007/0195>, 2007.
- 345 Stawiarski, C., Träumner, K., Knigge, C., and Calhoun, R.: Scopes and Challenges of Dual-Doppler Lidar Wind Measurements—An Error Analysis, *J. Atmos. Oceanic Technol.*, 30, 2044–2062, <https://doi.org/10.1175/JTECH-D-12-00244.1>, 2013.
- Tabas, D., Fang, J., and Porté-Agel, F.: Wind Energy Prediction in Highly Complex Terrain by Computational Fluid Dynamics, *Energies*, 12, 1311, <https://doi.org/10.3390/en12071311>, 2019.
- 350 van Dooren, M. F., Campagnolo, F., Sjöholm, M., Angelou, N., Mikkelsen, T., and Kühn, M.: Demonstration and uncertainty analysis of synchronised scanning lidar measurements of 2-D velocity fields in a boundary-layer wind tunnel, *Wind Energy Science*, 2, 329–341, <https://doi.org/10.5194/wes-2-329-2017>, available at: <https://www.wind-energ-sci.net/2/329/2017/wes-2-329-2017.pdf>, 2017.
- Vasiljević, N., Harris, M., Tegtmeier Pedersen, A., Rolighed Thorsen, G., Pitter, M., Harris, J., Bajpai, K., and Courtney, M.: Wind sensing with drone mounted wind lidars: proof of concept, 2019.
- 355 Vasiljević, N., L. M. Palma, J. M., Angelou, N., Carlos Matos, J., Menke, R., Lea, G., Mann, J., Courtney, M., Frölen Ribeiro, L., and M. G. C. Gomes, V. M.: Perdigão 2015: methodology for atmospheric multi-Doppler lidar experiments, *Atmos. Meas. Tech.*, 10, 3463–3483, <https://doi.org/10.5194/amt-10-3463-2017>, 2017.